Corrosion Science 90 (2015) 597–605

Contents lists available at ScienceDirect

Corrosion Science

journal homepage: www.elsevier.com/locate/corsci

The effects of microstructural factors on the corrosion behaviour of Mg–5Sn–*x*Zn (*x* = 1, 3 wt%) extrusions

Chang Dong Yim [a,b,*], Jie Yang [b], Sang Kyu Woo [b], Heon-Young Ha [a], Bong Sun You [a,b]

[a] Korea Institute of Materials Science, 797 Changwondae-ro, Seongsan-gu, Changwon, Gyeongnam 642-831, Republic of Korea
[b] University of Science and Technology, 217 Gajeong-ro, Yuseong-gu, Daejeon 305-350, Republic of Korea

ARTICLE INFO

Article history:
Received 4 July 2014
Accepted 1 November 2014
Available online 8 November 2014

Keywords:
A. Magnesium
A. Tin
A. Zinc
B. Polarisation
B. Weight loss

ABSTRACT

The effects of microstructural factors, including fraction of second phase particles and solute content in a matrix, on the corrosion behaviour of Mg–5Sn–*x*Zn (*x* = 1, 3 wt%) alloys were evaluated by using potentiodynamic polarisation and immersion tests. The hydrogen evolution rate and the corrosion potential increased with increasing Zn content, while the passive current density decreased. The average corrosion rate measured by immersion test increased with increasing Zn content, and was consistent with the hydrogen evolution rate. The increase of the corrosion rate with increasing Zn content resulted from increasing fraction of Mg_2Sn particles and Zn content dissolved in the matrix.

1. Introduction

Magnesium alloy has many advantages as a lightweight structural material, such as high specific strength, good damping capacity, castability and machinability [1,2]. Nonetheless, industrial application of magnesium alloy has been limited by its relatively low absolute strength and its poor corrosion resistance. It is well known that precipitation hardening is the most effective method to increase the strength of wrought alloys. The Mg–Sn system is known as a precipitation system, which has a relatively high solubility limit at 834 K and a low solubility at ambient temperature [3]. Even though the Mg–Sn system has great potential as a high strength wrought alloy via precipitation hardening, thus far its slow age hardening response has limited the practical application of Mg–Sn system alloys. Adding alloying elements as a means to enhance the age hardening response of Mg–Sn system alloys has been studied extensively [3–8]. According to previous reports, Zn has been an effective alloying element for improving the age hardening response of the Mg–Sn system alloys and for a more uniform distribution of fine Mg_2Sn particles [9–14].

A previous study reported that Sn has a relatively higher hydrogen evolution overpotential and, thus, the cathodic hydrogen evolution was relatively difficult on its surface [15]. Liu et al. [16] reported that the mode and rate of corrosion of Mg–7Sn binary alloy were dependent on the quantity of Mg_2Sn particles and Sn content in a matrix. They observed that the corrosion mode changed from pitting corrosion to filiform corrosion when the Mg_2Sn particles decomposed and most of the Sn was dissolved into a matrix by heat treatment at an elevated temperature, which resulted in the decrease of corrosion rate. Ha et al. [17] investigated the influences of metallurgical factors, including the volume fraction of Mg_2Sn particles, Sn content dissolved in a matrix, and the area fraction of grain boundaries, on the corrosion behaviour of Mg–*x*Sn binary alloy extrusions. They reported that the overall corrosion behaviour of Mg–*x*Sn alloys was strongly dependent on the volume fraction of Mg_2Sn particles, which promoted passivity, notably increased the hydrogen evolution rate, and acted as a pitting corrosion initiation site.

Other studies reported that Zn solutionised in a matrix increased the hydrogen evolution rate [18,19]. Ha et al. [19] reported that a faster hydrogen evolution rate in the alloy containing a higher Zn content resulted from the higher conductivity of ZnO. They also reported that the corrosion behaviour of single phase Mg–*x*Zn binary alloys was sensitive to immersion time. In the early stage of immersion, $Zn(OH)_2$ formed on the surface, and the fraction of $Zn(OH)_2$ increased with increasing Zn content. The formation of $Zn(OH)_2$ did not effectively protect the surface; therefore, $i_{passive}$ (passive current density) increased with increasing Zn content. By increasing the immersion time, the $Zn(OH)_2$ was c hanged gradually to stable ZnO, which could enhance the protectiveness of the surface film. Therefore, the $i_{passive}$ decreased with

* Corresponding author at: Korea Institute of Materials Science, 797 Changwondae-ro, Seongsan-gu, Changwon, Gyeongnam 642-831, Republic of Korea. Tel.: +82 55 280 3530.
E-mail address: cdyim03@kims.re.kr (C.D. Yim).

http://dx.doi.org/10.1016/j.corsci.2014.11.003
0010-938X/

increasing Zn content. Song et al. [20] also reported that the passivity of the film that formed on the surface of Mg–xZn binary alloys was dependent on the condition to which the corrosive media were exposed.

According to the previous studies, the Mg–Sn–Zn system has great potential to produce a high strength and highly corrosion resistant wrought alloy. Although many studies on the mechanical behaviours of this alloy system have been conducted, few studies focused on the corrosion behaviour of the Mg–Sn–Zn system have been carried out. In this study, the corrosion behaviour of a magnesium alloy containing Sn and Zn was evaluated via potentiodynamic and immersion tests. The change of corrosion behaviour according to the composition of the alloy was analyzed with respect to its microstructure.

2. Experimental procedure

2 kg of pure magnesium ingot was put into a carbon crucible and heated to 973 K by induction heating under a protective atmosphere of CO_2 and SF_6 gases. Pure tin (99.99%) and pure zinc (99.99%) granules were added into the melt according to the given composition. The melt was poured into a cylindrical mould that was preheated to 473 K. The compositions of the alloys were analyzed by an inductively coupled plasma as shown in Table 1. A homogenisation heat treatment was carried out for 24 h at 723 K to homogenise the microstructure of the as-cast billets, and the homogenisation temperature was determined in accordance with the phase diagram shown in Fig. 1. This phase diagram was calculated using Pandat [21], commercial software for thermodynamic calculation. After homogenisation, the original billets were machined into billets with dimensions of 78 mm in diameter and 145 mm in length for extrusion. The machined billets were preheated to 573 K for 3 h and then extruded indirectly through a rectangular die having dimensions of 2 mm in thickness and 28 mm in width. The die and container were also preheated to 573 K. The extrusion ratio and speed were 90:1 and 5.0 m/min, respectively.

The specimens prepared for microstructure observation were cut from the as-extruded plates and mounted using epoxy resin. Each mounted specimen was mechanically ground using #240–#2400 grit SiC papers and then polished using pastes containing diamond particles of 3 μm, 1 μm and 0.25 μm. Each polished specimen was etched using a solution of 3 g picric acid, 20 ml acetic acid, 20 ml distilled water, and 50 ml ethanol to reveal the microstructure more clearly. The microstructures of as-extruded TZ5x alloys were observed using an optical microscope (Nikon Optiphot 200) and a scanning electron microscope (SEM; JSM-6610, JEOL) equipped with an energy dispersive X-ray spectroscopy (EDS). The constituent phases of the as-extruded TZ5x alloys were analyzed by measuring the X-ray diffraction pattern using an X-ray diffractometer (XRD; D/Max-2500VL/PC, Rigaku). The scanning range of 2θ was from 20° to 80° and the scanning speed was 2°/min.

The electrochemical behaviour of the as-extruded TZ5x alloys was evaluated via potentiodynamic test using a potentiostat (VersaSTAT 4, Princeton Applied Research). Specimens of 16 mm in diameter and 2 mm in thickness were machined from the as-extruded plates and then ground mechanically using #240–#2400 grit SiC papers. Each specimen was inserted into a holder and then put into a flask containing a 3.5 wt% NaCl solution at 298 K. A three-electrodes array was applied to the potentiodynamic test. The working electrode, reference electrode, and counter electrode were the specimen, a saturated calomel electrode, and a carbon rod, respectively. The open circuit potential (OCP) was measured over 3600 s, and then the external voltage was changed from −0.25 V to 0.5 V with respect to an OCP at rate of 1 mV/s. The potentiodynamic test was stopped when the current density reached 0.01 mA/cm^2, even though the external voltage did not reach 0.5 V with respect to the OCP. The electrochemical tests were conducted at least three times, and good reproducibility was confirmed.

Table 1
Chemical composition of TZ5x alloys (wt%).

Alloy	Sn	Zn	Si	Ca	Fe	Mg
TZ51	4.56	1.06	0.021	0.0080	0.0010	Bal.
TZ53	4.69	3.15	0.021	0.0047	0.0017	Bal.

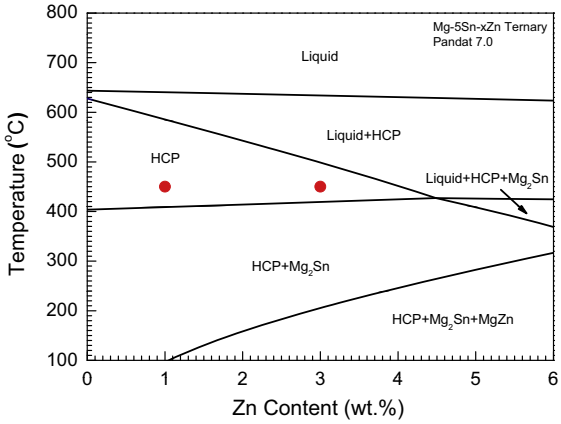

Fig. 1. Phase diagram of Mg–5Sn–xZn ternary system.

The average corrosion rates were measured using immersion test. Specimens of 28 mm in width, 36 mm in length, and 2 mm in thickness were machined from the as-extruded plates and then ground mechanically using #240–#2400 grit SiC papers. The specimens for the immersion test were put into a 3.5 wt% NaCl solution, and the temperature of the solution was maintained isothermally at 298 K using an isothermal control chamber. After immersion for 72 h, the corrosion products on the surface were removed using a solution of 200 g/l CrO_3 and 10 g/l $AgNO_3$. Weight loss before and after immersion test was measured and converted to the average corrosion rate according to ASTM G1-03. The corrosion rate was determined as the average value of the three test results and the standard deviation was expressed as an error bar.

3. Results and discussion

Fig. 2 shows the microstructures of as-cast and as-extruded TZ5x alloys. The as-cast alloys showed a typical dendritic structure. The dendritic arm was more distinctly developed with increasing Zn content due to constitutional undercooling by segregation of Zn at the solid/liquid interface during solidification [22]. Second phases formed during solidification were clearly observed in grain interiors and along grain boundaries. Table 2 shows the results of the thermodynamic calculation for the mole fractions of the 2nd phases formed during solidification of TZ5x alloys. As shown in Table 2, the formation of Mg_2Sn, BCC_B2 (Fe-rich FeSiMgZn compound), Ca_2Sn_X (Ca_2Sn compound containing Mg), Mg_2Si_X (Mg_2Si compound containing Sn), BCC (Fe-rich FeZnMgSnSiCa compound) and MgZn phases was predicted due to the inclusion of Si, Ca and Fe as impurities in the raw materials. The increase of mole fractions of Mg_2Sn and MgZn phases was predicted with increasing Zn content, and was consistent with the increase of black areas surrounding α-Mg grains. The complete dissolution of the Mg_2Sn, BCC and MgZn phases was predicted during homogenisation at 723 K as shown in Table 3.